Chapter 3
Stress Concentration at Notches

3.1 Introduction

Calculations on the strength of structures are primarily based on the theory of elasticity. If the yield stress is exceeded plastic deformation occurs and the more complex theory of plasticity has to be used. Fatigue, however, and also stress corrosion, are phenomena which usually occur at relatively low stress levels, and elastic behavior may well be assumed to be applicable. The macroscopic elastic behavior of an isotropic material is characterized by three elastic constants, the elastic modulus or Young's modulus (E), shear modulus (G) and Poisson's ratio (ν). The well-known relation between the constants is $E = 2G(1 + \nu)$.

In a structure, geometrical notches such as holes cannot be avoided. The notches are causing an inhomogeneous stress distribution, see Figure 3.1, with a stress concentration at the "root of the notch". The (theoretical) stress concentration factor, K_t,[6] is defined as the ratio between the peak stress at the root of the notch and the nominal stress which would be present if a stress concentration did not occur.

[6] K_t is often referred to as the theoretical stress concentration factor. However, the factor is not a theoretical one. It is based on the assumption of linear elastic material behavior.

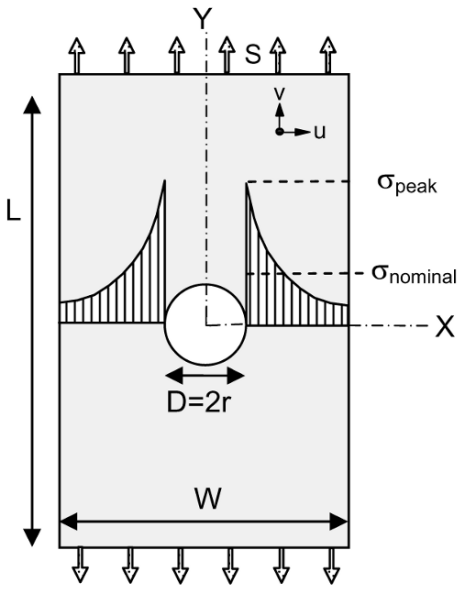

Fig. 3.1 Strip with central hole as a prototype of a notched part.

$$K_t = \frac{\sigma_{\text{peak}}}{\sigma_{\text{nominal}}} \tag{3.1}$$

The severity of the stress concentration is depending on the geometry of the notch configuration, generally referred to as the shape of the notch. Designers should always try to reduce stress concentrations as much as possible in order to avoid fatigue problems. The present chapter deals with various aspects of stress concentrations and the effect of the geometry (the shape) on K_t. This is one of the fundamental issues of designing a fatigue resistant structure, i.e. designing against fatigue. Problems discussed in the present chapter cover definitions of stress concentration factors, calculations and estimations of K_t-values, stress gradients, aspects related to size and shape effects, superposition of notches and methods to determine K_t-values.

3.2 Definition of K_t

The strip with a central hole shown in Figure 3.1 is a prototype of a notched element. It is frequently used in fatigue experiments to study notch effects on fatigue. If the strip is loaded by a homogeneous stress distribution, the hole will cause an inhomogeneous stress distribution in the critical section, which

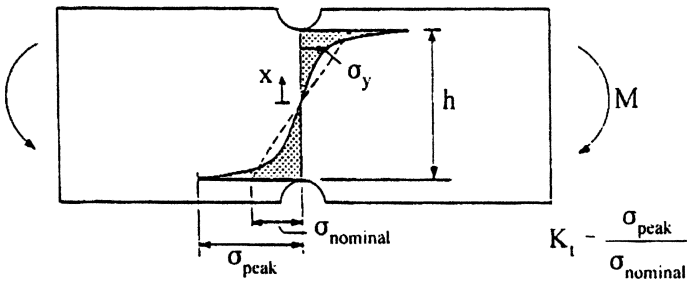

Fig. 3.2 Stress distribution in a beam with two grooves loaded in bending.

is the minimum section at the hole. This stress distribution is characterized by a peak stress σ_{peak} at the root of the notch, and a nominal net section stress σ_{nominal}. The ratio of the peak stress and the nominal stress in the net section leads to the commonly used definition of the stress concentration factor K_t given in Equation (3.1). It should be emphasized that all deformations are supposed to be elastic. K_t is essentially an elastic concept. It gives a direct indication of the severity of the stress concentration, because it is an amplification factor on the stress level which is nominally present in the net section of the notch.

$$\sigma_{\text{peak}} = K_t \, \sigma_{\text{nominal}} \tag{3.2}$$

Sometimes it is informative to see the ratio between the peak stress and the gross stress S, applied to the element. This ratio with the symbol K_{tg} is:

$$K_{tg} = \frac{\sigma_{\text{peak}}}{S} \tag{3.3a}$$

The two factors are obviously interrelated. With the dimensions W (specimen width) and D (hole diameter):

$$K_{tg} = \frac{\sigma_{\text{nominal}}}{S} K_t = \frac{W}{W - D} K_t \quad \text{and thus} \quad K_{tg} > K_t \tag{3.3b}$$

K_t and K_{tg} are the symbols used by R.E. Peterson in his book *Stress Concentration Factors* [1], which is a standard book on stress concentrations. In general, K_t is the preferred factor to indicate the stress concentration.

For bending and torsion the definition of K_t is the same as given in Equation (3.1); K_t is the ratio between the peak stress at the root of the notch and the nominal stress in the critical net section. The nominal stress for the strip with the side grooves in Figure 3.2 is the bending stress which would be present if the stress concentration did not occur:

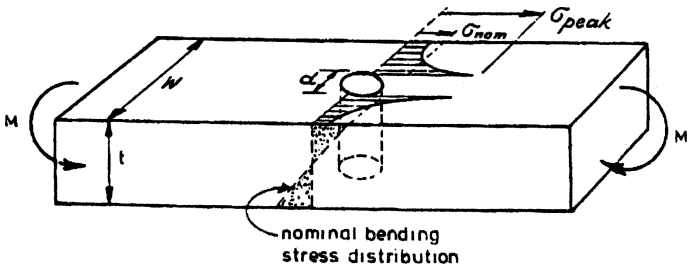

Fig. 3.3 Stress distribution in a beam with a transverse hole loading in bending.

$$\sigma_{\text{nominal}} = \frac{6M}{th^2} \tag{3.4}$$

(t = thickness of the beam; h = height of minimum section, see Figure 3.2).

The nominal stress for the strip with a transverse hole also loaded in bending shown in Figure 3.3 is:

$$\sigma_{\text{nominal}} = \frac{6M}{(W - D)t^2} \tag{3.5}$$

K_t-values can be obtained with different methods:

- by calculations: analytical methods, finite-element methods (FEM),
- by measurements: strain gage measurements, photo-elastic measurements.

Some comments on measurements versus calculations are given in Section 3.7.

3.3 Analytical calculations on stress concentrations

Analytical solutions based on the theory of elasticity are not treated in detail here. The analysis can be found in various textbooks (e.g. [2, 3]). Basically, the following procedure is used. For a two-dimensional problem, as shown in Figure 3.1, the displacement functions $u(x, y)$ and $v(x, y)$ have to be found. If these functions are obtained, the strains follow from these functions, and the stresses are linked to the strains by Hooke's law. The problem then is apparently solved. As part of finding the solution, the tensile strains, ε_x(x,y) and ε_y(x,y), and the shear strain $\gamma_{xy}(x, y)$ must satisfy the compatibility equation. Furthermore, there are equilibrium equations for σ_x, σ_y and τ_{xy}. These stresses are linked to the strains by three equations representing

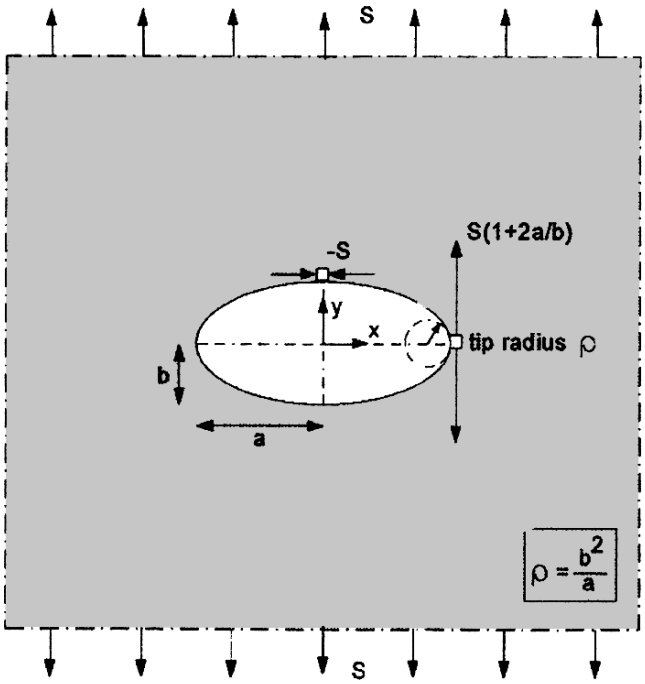

Fig. 3.4 Stress concentration of an elliptical hole in an infinite sheet.

Hooke's law, including the elastic constants of the material. The equations obtained are rewritten by introducing the Airy stress function ϕ which leads to a biharmonic equation. The problem then is to find a function ϕ that satisfies this equation. The solution will still contain unknown constants, which should follow from the boundary conditions. These conditions are essential for solving a particular problem. For the tensile strip with a central hole in Figure 3.1, the boundary conditions are:

1. At the upper and lower edge: $\sigma_y = S$, $\sigma_x = 0$, $\tau_{xy} = 0$.
2. At the side edges ($x = \pm W/2$): $\sigma_x = 0$, $\tau_{xy} = 0$.
3. At the edge of the hole: the stress perpendicular to the hole edge and the shear stress are zero.

An exact analytical solution for the apparently simple case of Figure 3.1, a strip with a hole, is not available, but accurate numerical approximations were obtained. However, for an infinite sheet with an elliptical hole the exact solution was obtained [2, 3]. This problem is known as a classical problem in the theory of elasticity. It is not really a simple problem. Elliptical coordinates and complex functions are used to arrive at the solution, which

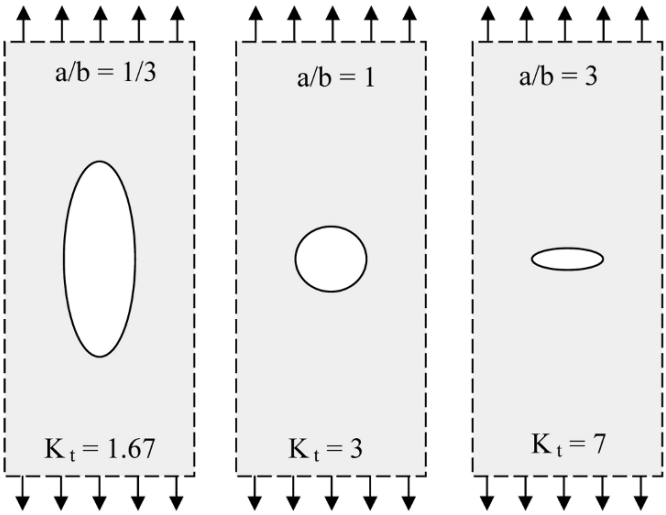

Fig. 3.5 Effect of the shape of the hole on K_t, infinite sheet under tension (Figure 3.4).

then provides the stress distribution in the entire plate. The results illustrate several interesting features of stress distributions around the hole. The tangential stresses along the edge of the hole are of great interest. The maximum stress, σ_{peak}, occurs at the end of the main axis ($x = a$, $y = 0$), see Figure 3.4. The semi-axes of the elliptical hole are a and b respectively. The tip radius at the end of the major axis follows from $\rho = b^2/a$. The equations for the peak stress and K_t are simple:

$$\sigma_{\text{peak}} = S\left(1 + 2\frac{a}{b}\right) = S\left(1 + 2\sqrt{\frac{a}{\rho}}\right) \tag{3.6a}$$

$$K_t = 1 + 2\frac{a}{b} = 1 + 2\sqrt{\frac{a}{\rho}} \tag{3.6b}$$

The last equation indicates that a small notch root radius ρ will give a high K_t, whereas a large radius will give a low K_t. This is illustrated in Figure 3.5. Although a structure is not directly comparable to a sheet with an elliptical hole, it is always profitable to use large radii in notched components to reduce the stress concentration.

A circular hole is a special case, obtained from an ellipse with equal axes; $a = b$. The K_t-value according to Equation (3.6b) is equal to 3. This is a classical value. For an open hole in a structural part, the K_t-value will be somewhat lower because the component has a finite width. In practice, fatigue cracks have indeed frequently occurred in structures at open holes.

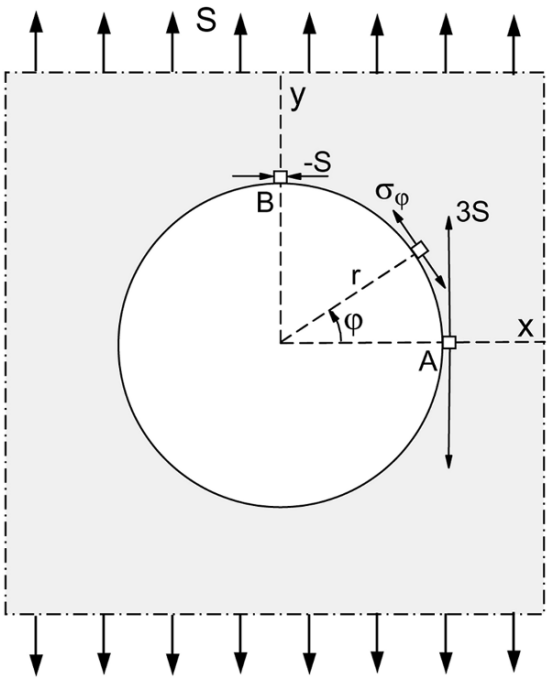

Fig. 3.6 Tangential stress around a circular hole in a sheet loaded by a remote tensile stress S.

It is noteworthy that the tangential stress at the end of the vertical axis ($y = b$, $x = 0$ in Figure 3.4) is a compressive stress, which is equal to the tensile stress applied to the infinite plate. This result is valid for all ellipses, and thus also for a circular hole, see Figure 3.6. Along the edge of the hole, starting from A to the top of the hole B the tangential stress changes from $+3S$ to $-S$, following the equation:

$$\sigma_\varphi = S(1 + 2\cos 2\varphi) \tag{3.7}$$

The value of the tangential stress must go through zero ($\sigma_\varphi = 0$) which occurs at $\varphi = 60°$.

Stress gradients

Although the peak stress is of great importance, it is also interesting to know how fast the stress decreases away from the root of the notch, see Figure 3.7. The stress gradient of σ_y along the X-axis is used in some prediction models

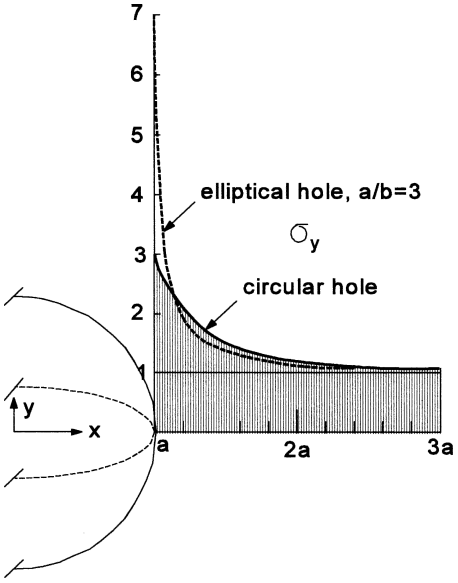

Fig. 3.7 Stress gradients are high at the root of the notch.

to account for the size effect on the fatigue limit of notched parts. For an elliptical hole in an infinite sheet, the exact solution for σ_y along the X-axis is given by:

$$\frac{(\sigma_y)_{y=0}}{S} = 1 + \frac{a(a-2b)(x-\sqrt{x^2-c^2})(x^2-c^2) + ab^2(a-b)x}{(a-b)^2(x^2-c^2)\sqrt{x^2-c^2}} \tag{3.8}$$

where $c^2 = a^2 - b^2$. For $x = a$, the equation reduces to Equation (3.6b). For x very large, the asymptotic result is $(\sigma_y)_{y=0} = S$ as should be expected far away from the hole.

For a circular hole, Equation (3.8) becomes more simple:

$$\frac{(\sigma_y)_{y=0}}{S} = 1 + \frac{1}{2}\left(\frac{a}{x}\right)^2 + \frac{3}{2}\left(\frac{a}{x}\right)^4 \tag{3.9}$$

The distributions of $(\sigma_y)_{y=0}$ for a flat elliptical hole ($a/b = 3$, $K_t = 7$) and for a circular hole are given in Figure 3.7. Obviously, the peak stress drops off much faster for the higher peak stress of the elliptical hole. The stress gradient of $(\sigma_y)_{y=0}$ at the root of the notch ($x = a$) is obtained by differentiation of Equation (3.8). With $K_t = 1 + 2a/b$ (Equation 3.6b), the gradient can be written as

$$\left(\frac{\mathrm{d}\sigma_y}{\mathrm{d}x}\right)_{x=a} = -\left(2 + \frac{1}{K_t}\right)\frac{\sigma_{\text{peak}}}{\rho} = -\alpha\frac{\sigma_{\text{peak}}}{\rho} \tag{3.10}$$

The negative gradient is proportional to the peak stress (expected for linear elastic behavior) and inversely proportional to the root radius. The proportionality constant is:

$$\alpha = 2 + \frac{1}{K_t} \tag{3.11a}$$

which implies

$$2 < \alpha < 3 \tag{3.11b}$$

Apparently, K_t does not have a large effect on the stress gradient coefficient α. For notches in a structure with K_t in the range of 2 to 5, the value of α is about 2.2 to 2.5 [5].

The stress gradient at the root of a notch should give an indication of the volume of the highly stressed material. As a numerical example, an estimate is made of the distance δ along the X-axis for drop of σ_y from σ_{peak} to $0.9\sigma_{\text{peak}}$, a drop with 10%. A circular hole ($K_t = 3.0$) with a diameter of 5 mm ($\rho = 2.5$ mm) is considered. Assuming a linear stress gradient, the value of δ can be derived with Equation (3.10):

$$\left(\frac{\mathrm{d}\sigma_y}{\mathrm{d}x}\right)_{x=a} \approx -\frac{\sigma_{\text{peak}} - 0.9\sigma_{\text{peak}}}{\delta} = -\left(2 + \frac{1}{3}\right) \cdot \frac{\sigma_{\text{peak}}}{2.5}$$

which gives $\delta \approx 0.1$ mm $= 100$ μm. For an average grain size of 50 μm the depth δ corresponds to just a few grains. Conclusion: Especially the grains at the notch root surface are the highly loaded grains. This is important for fatigue.

The stress gradient along the edge of the notch

In the previous paragraphs, it was discussed how σ_y is dropping off away from the edge of the hole. However, in Chapter 2 it was pointed out that fatigue crack nucleation is a surface phenomenon. It then appears to be of interest to know how fast the tangential stress along the notch edge is decreasing. This is illustrated by Figure 3.8, again for a circular hole. Lines of a constant principal stress were calculated for stress levels of 95, 90, 80 and 50% of the peak stress. The 90% line corresponds to a 10% reduction of the peak stress. An interesting result should be noted. The tangential stress along the edge of the hole decreases relatively slowly in comparison to the stress away from the edge (along the X-axis). It then should be recalled that crack nucleation starts at the material surface. Apparently, the highly stressed

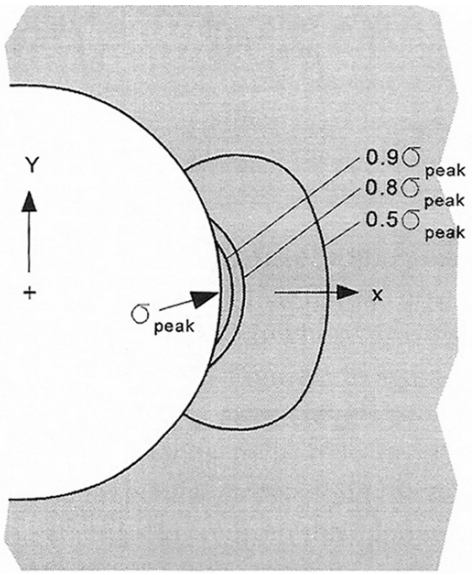

Fig. 3.8 Relatively slow decrease of the stress along the edge of a notch, illustrated by lines of constant principal stress for a circular hole loaded in tension [5].

surface layer is stretched along the edge of the hole. It implies that the stress gradient along the edge of the hole is of greater importance than the stress gradient perpendicular to the hole edge.

Larger notches have a larger material surface along the root of the notch, which is significant for the notch size effect on fatigue to be discussed in Chapter 7. Furthermore, the extent of the highly stressed material along the wall of a hole emphasizes the significance of the surface quality obtained in the production. This topic is also discussed in Chapter 7.

The calculated results discussed above were obtained for an infinite sheet with an elliptical hole, and with a circular hole as a special case. More results presented in [5] indicate that the trends with respect to the stress gradients are more or less similar for all notches in the engineering range of relevant K_t-values and notch root radii. Similar peak stresses and notch root radii give comparable stress distributions around the root of the notch, and the trends discussed in this section are thus valid for engineering design considerations.

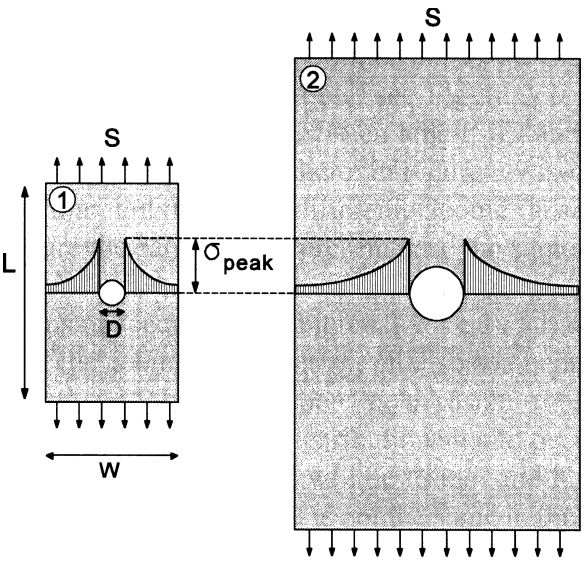

Fig. 3.9 Geometrically similar specimens have the same K_t, but different stress gradients.

3.4 Effect of the notch geometry on K_t

For a circular hole in an infinite sheet, the only dimension is the diameter D. However, for the simple tension specimen with a central hole, see Figure 3.1, there are already three dimensions: the specimen width (W), the specimen length (L) and the hole diameter (D). The specimen thickness is not yet considered here. In Figure 3.9 two specimens are shown, which are geometrically similar, but the size is different. Geometric similarity implies that all ratios of the dimensions are the same, in the present case the same D/W and L/W.

Because K_t is a dimensionless ratio, it can depend on dimensionless geometrical ratios only. Assume that all dimensions of specimen 2 in Figure 3.9 are two times larger than the dimension of specimen 1. As a result of the geometric similarity, all displacements are also two times larger, but the relative displacements will be the same. As a result, the strains are the same. Consequently, a geometrically similar stress distribution should occur in both specimens as depicted in Figure 3.9. The same peak stress will be found, and K_t is the same. However, due to the difference in size, the stress gradient is not the same in the two specimens because the gradient is not dimensionless. According to Equation (3.10), the gradient is inversely proportional to the root radius ρ. The consequence is that larger

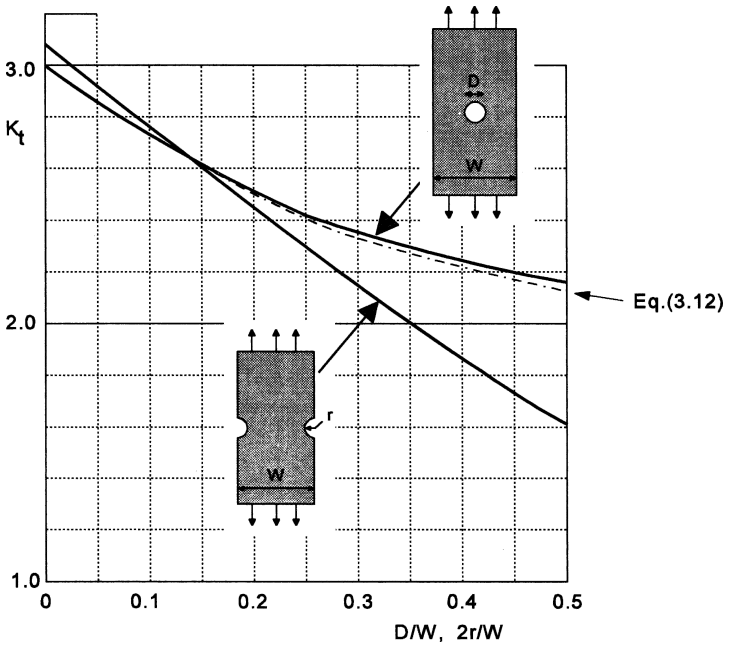

Fig. 3.10 K_t for a specimen with a central hole and a specimen with two edge notches [1].

specimens have larger volumes and larger notch surface areas of highly stressed material, which is significant for the size effect on fatigue.

Many K_t graphs for various shapes and different types of loading can be found in the book by Peterson [1]. Collections of K_t-values are also presented in other sources, e.g. in the ESDU Data Sheets [4]. Furthermore, software packages also containing a K_t database are now commercially available. Some simple examples of K_t graphs will be shown here to illustrate the effect of the shape on the stress concentration. Figure 3.10 shows K_t for a central hole and a double edge notch, geometries frequently adopted for fatigue investigations in laboratories. For an increasing notch radius (r) the value of K_t decreases, although much more for the edge notched specimen than for the central hole specimen. For the edge notched specimen $K_t \rightarrow 1$ for $2r/W \rightarrow 1$ (zero ligament between the notches), while for the central hole specimen $K_t \rightarrow 2$ for $D/W \rightarrow 1$ (also zero ligaments).

The $K_t(D/W)$ curve for the central hole specimen, based on calculations of Howland [6], was approximated by Heywood [7] by Equation (3.12) to:

$$K_t = 2 + \left(1 - \frac{D}{W}\right)^3 \tag{3.12}$$

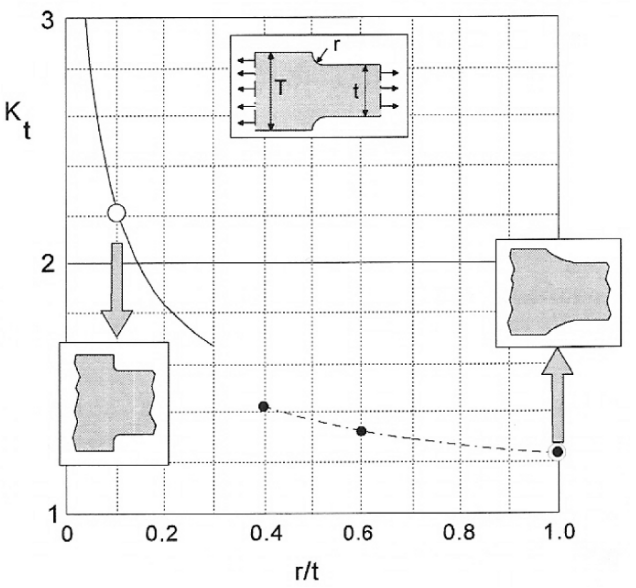

Fig. 3.11 K_t for a fillet, $t/T = 2/3$. Data from two graphs in [1].

The value of K_t should also depend on the length of the specimen, but this influence is negligible if the length is more than twice the specimen width.

Another illustration is given in Figure 3.11 for a fillet where the plate thickness (T) is reduced to a lower thickness (t) with a transition radius r. In this case two geometric ratios have to be considered, e.g. t/T and r/t. Figure 3.11 applies to a single value of the thickness reduction ratio t/T ($= 2/3$). The graph shows K_t as a function of r/t as obtained from two different sources. The two curves suggest some disagreement because the $K_t(r/t)$ function appears to be discontinuous which cannot be correct. In spite of some inaccuracies of the curves, Figure 3.11 clearly illustrates that a larger radius leads to a significantly smaller K_t, see the two inset figures for $r/t = 0.1$ and 1.0 respectively. The corresponding K_t-values are 2.24 and 1.24, which means a 45% lower K_t for the larger root radius.

It is also instructive to see how the K_t-values compare for different shapes with the same geometry ratios, see Figure 3.12. The highest K_t-value in this figure applies to the edge notches. The fillet geometry is obtained by removing material from the edge notch geometry. K_t is then reduced by 25%. The fillet geometry is less disturbing for the "stress flow". The stress flow can be visualized by the main principal stress trajectories, which have to bend around the notch, see Figure 3.13. Thinking in terms of the stress

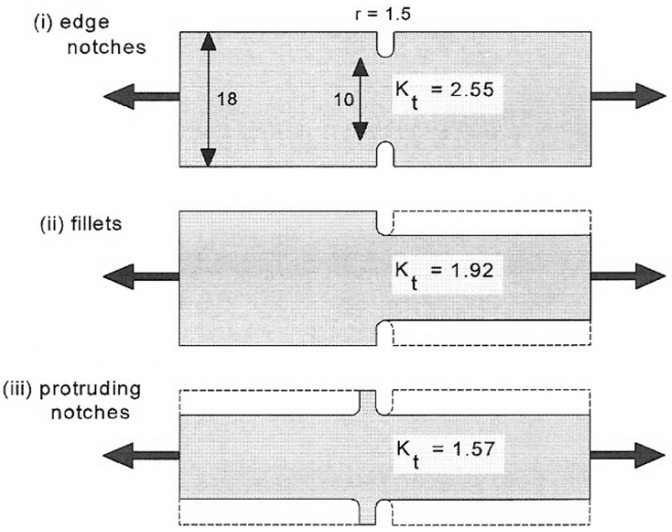

Fig. 3.12 Three geometries with the same root radii but with different stiffness transitions. K_t-values derived from graphs in [1].

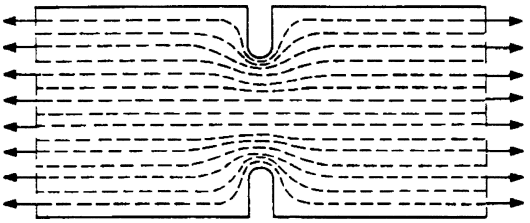

Fig. 3.13 Main principal stress trajectories bending around the notch.

flow, it could be qualitatively expected that the fillet in Figure 3.12, case (ii), does not obstruct the stress flow as much as the edge notch. The third case in Figure 3.12 is derived from the fillet case by a further omission of material, leaving two external ledges. Such a protruding notch has a limited effect on the stress flow, which reduces K_t still further. The highest K_t-value in Figure 3.12 is obtained for the intruding notch, which applies also to intruding damage to the surface material, such as dents, corrosion pits or imprinted letter codes of the manufacturer. An illustration of a corrosion pit with an estimated K_t-value is given in Figure 3.14. The effect of corrosion pits on the S-N curve was discussed in Chapter 2, see Figure 2.28.

The effect of the root radius on K_t is again illustrated by Figure 3.15 for a shaft with a shoulder fillet. Values are given for a diameter reduction $d/D = 2/3$, for two loading cases; tension and bending. The K_t-values

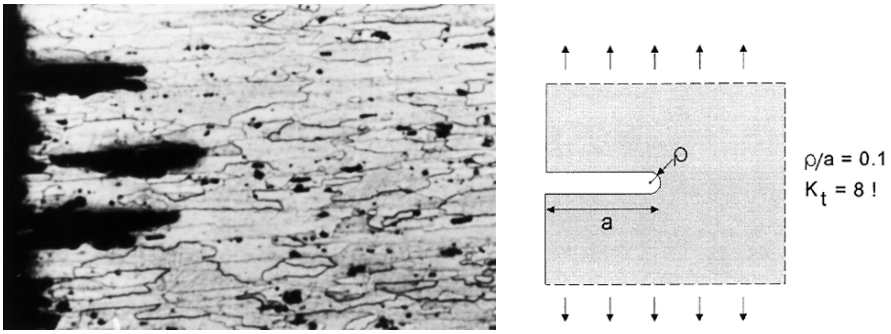

Fig. 3.14 Relative deep corrosion pits in a so-called end grain structure at the material surface of an aluminium alloy part. Pit depth = 0.15 mm. The geometrically equivalent shape leads to a very high K_t.

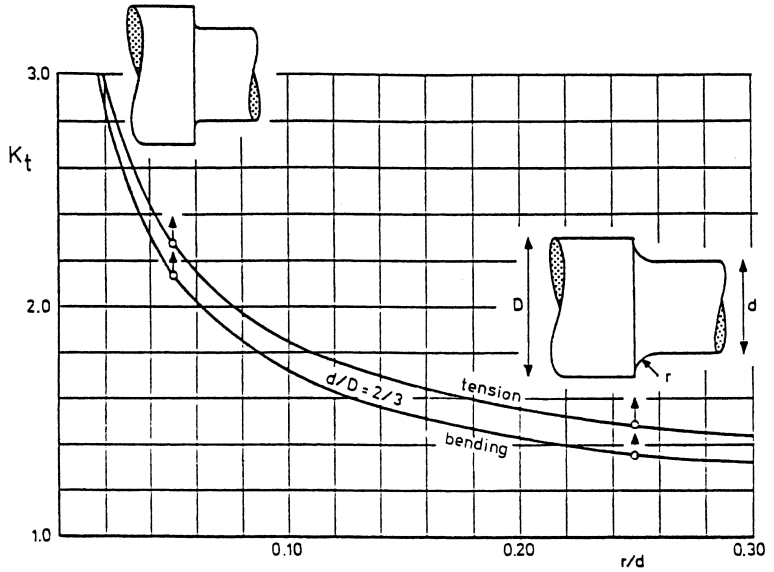

Fig. 3.15 The effect of the root radius of a shoulder on K_t. Results derived from [1].

for bending are slightly smaller than for tension. Similar to the graph for fillets in Figure 3.11, it illustrates that fairly low K_t-values can be obtained provided that a "generous" root radius is adopted. However, this is not always possible in practice, for instance if a ball bearing has to support a shaft as shown in Figure 3.16. The radius at the fillet can then be increased by a stress relieving groove in the shoulder of the thicker part, which reduces the stress concentration.

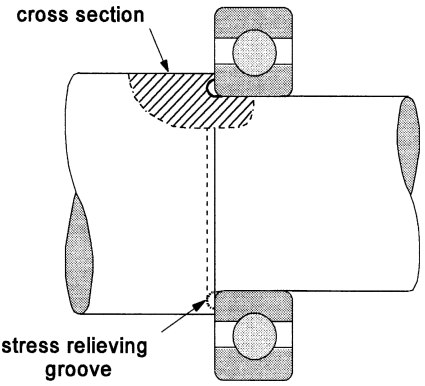

Fig. 3.16 Stress relieving groove by increasing the root radius at a shoulder.

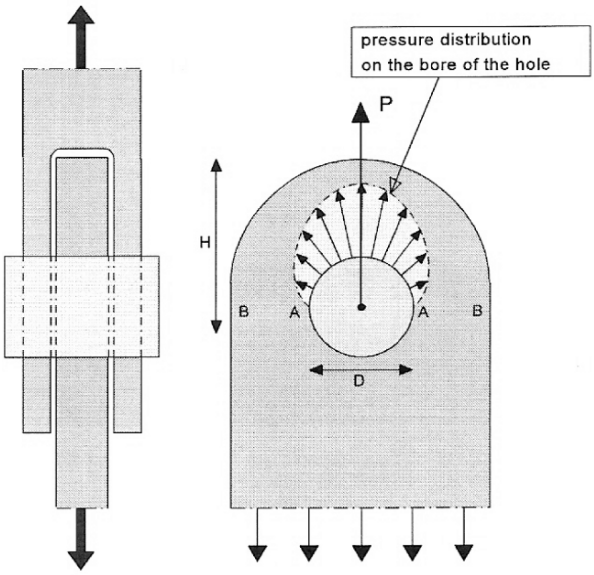

Fig. 3.17 Lug type joint with a pin-loaded hole.

Pin-loaded hole

The most elementary case of a pin-loaded hole is the connection between a lug (or lug head) and a clevis, see Figure 3.17. Load transmission between the lug and fork occurs by a single pin or a bolt. The pin applies a distributed pressure load to the upper half of the bolt hole in the lug. In many practical cases it is essential that some rotation in the joint is possible, which requires a clearance fit between the bolt and the hole and no clamping between the fork

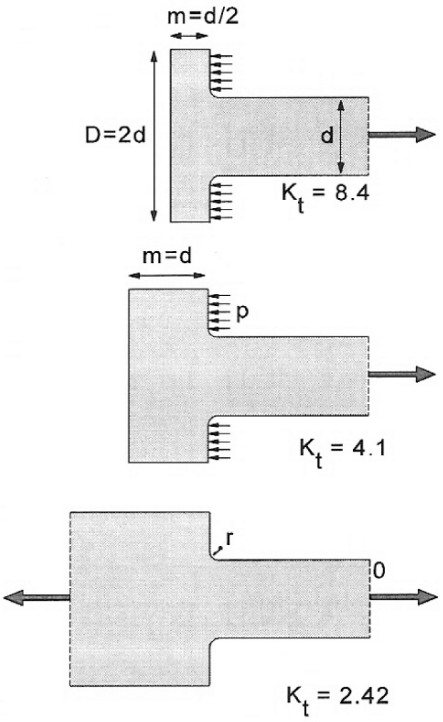

Fig. 3.18 High K_t-values of the flat T-heads with pressure loads close to the root on the notch ($r/d = 0.1$). Comparison to fillet.

and lug. For the critical net section of the lug (B-B in Figure 3.17), it implies pressure loads on the hole in the near vicinity of the root of the notch (points A in Figure 3.17), which is the location where crack nucleation should be expected under cyclic loading. This proximity of pressure on the hole surface and the critical section usually leads to relatively high stress concentrations. An elementary illustration of this observation is given in Figure 3.18 for a so-called T-head. In this case, the load P is balanced by a surface pressure p on the head edges, which is close to the root of the notch. For the two T-heads, K_t is significantly higher than for the fillet where no pressure loads in the vicinity of the notch root are present. Note also the difference between the two T-heads with the same radius ($K_t = 8.4$ and $K_t = 4.1$ respectively). The high K_t-value in the upper case of Figure 3.18 is associated with the lower bending stiffness of the T-head.

Values of K_t for lugs are the wellknown results obtained by Frocht and Hill from photo-elastic measurements [8]. These results are presented in

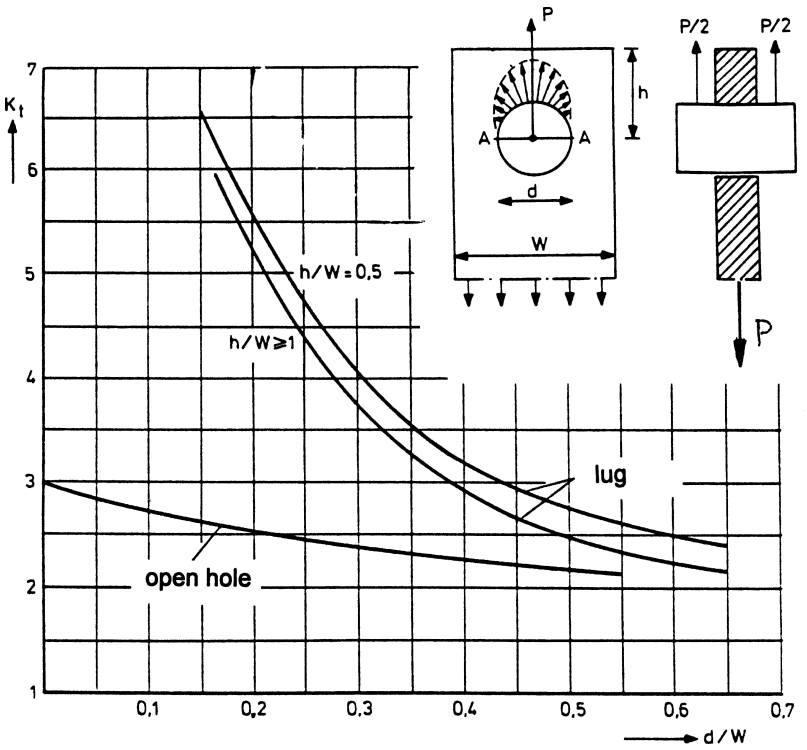

Fig. 3.19 K_t-values for a lug. Results of Frocht and Hill [8]. Comparison to an open unloaded hole.

Figure 3.19 in comparison to K_t-values for an open unloaded hole. The pin-loaded hole obviously causes the more severe stress concentration. This should be associated with the pressure load distribution applied closely to the root of the notch as mentioned earlier. In view of the high K_t-values, lugs are fatigue critical parts, but that is also due to fretting corrosion occurring inside the hole to be discussed in Chapter 15. Values of D/W below 1/3 are generally avoided to keep K_t-values below about 3.5.

3.5 Some additional aspects of stress concentrations

Pure shear

The stress concentration factor for a circular hole in a plate under pure shear loading can be obtained by superposition of two uniaxial loading cases, see

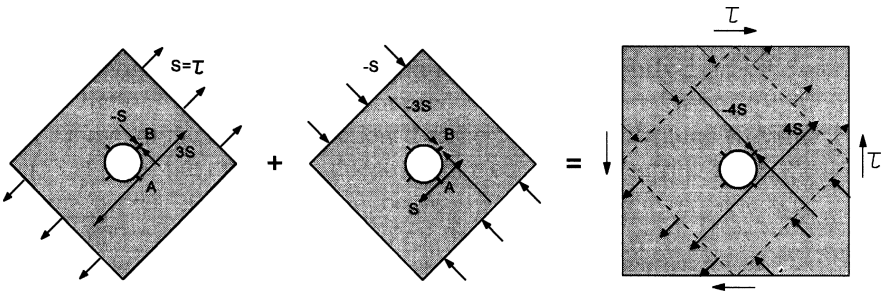

Fig. 3.20 K_t for pure shear obtained by superposition of two cases.

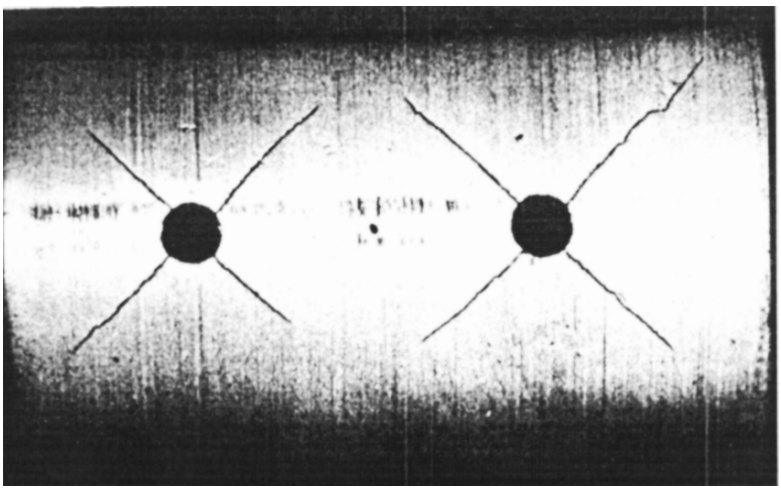

Fig. 3.21 Fatigue craks growing from holes in a shaft subjected to cyclic torsion. Material low-C steel [9].

Figure 3.20. Pure shear can be split into a pure tension case S at 45° and a pure compression case $-S$ at $-45°$. Summing the stresses at points A and B lead to tangential stresses of $4S$ and $-4S$. Because $S = \tau$, it leads to $K_t = 4$, quite a high value. Fatigue cracks have indeed been observed under cyclic torsion at the critical points at $\pm 45°$, see Figure 3.21.

Biaxial loading

Another simple case is the stress concentration of an elliptical hole under biaxial loading, as shown in Figure 3.22. The tangential stresses at the ends of the two axes of the elliptical hole are obtained by superposition of the two mutually perpendicular load cases, S and βS, with β as the biaxiality ratio.

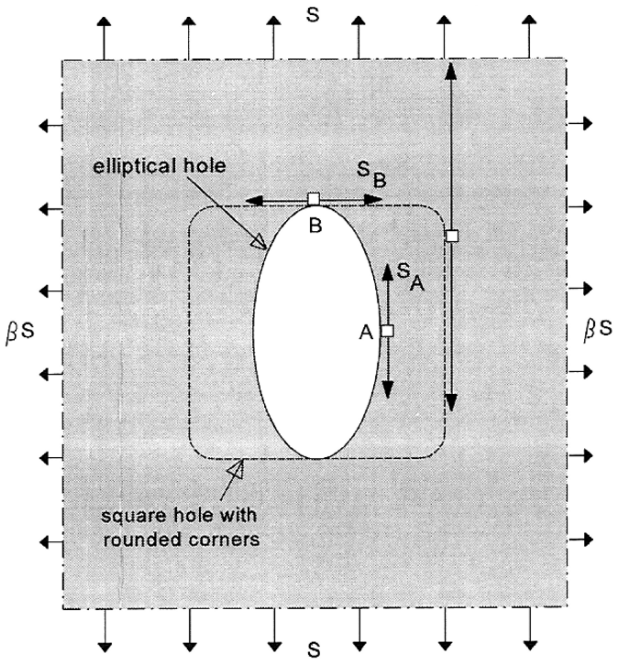

Fig. 3.22 Elliptical hole in biaxial stress field.

With the stress values presented earlier in Figure 3.4, the following equations are obtained:

$$\begin{aligned} &\text{Point A:} \quad S_A = S(1 + 2a/b) - \beta S \\ &\text{Point B:} \quad S_B = \beta S(1 + 2b/a) - S \end{aligned} \tag{3.13}$$

The biaxiality in the shell of a pressure vessel is due to the circumferential hoop stress and the longitudinal tension stress. The ratio is $\beta = 0.5$ if stiffeners are not present. For this ratio and a circular hole ($a = b$), substitution in Equation (3.13) gives:

$$S_A = 2.5S \quad \text{and} \quad S_B = 0.5S$$

The value of S_A is lower than $3S$ applicable to uniaxial loading. The biaxiality relieves the stress concentration. However, a further reduction is possible for an elliptical hole. If the b/a ratio is chosen to be 2, and again $\beta = 0.5$, see Figure 3.22, the result with Equation (3.13) is:

$$S_A = 1.5S \quad \text{and} \quad S_B = 1.5S$$

or $S_A = S_B$. Actually, the tangential stress in the latter case is equal to $1.5S$ along the full edge of the hole.

A completely different type of hole is also indicated in Figure 3.22. The dashed line represents a square hole with rounded corners (radius is 10% of hole width). For the same biaxiality ($\beta = 0.5$) the K_t-value for this hole is 4.04 [1], a large difference as compared to the elliptical hole. Of course it should be realized that these results are theoretical results, because open holes in a pressure vessel cannot exist. However, they illustrate that shapes can have a large effect on the stress concentrations. Designers nowadays can avoid undesirable shapes more easily than in the past by using computer controlled machining techniques.

Reinforcements of open holes

In various structures, openings cannot be avoided for several reasons associated with the usage of the structure. Approximately rectangular openings can be desirable in large shell structures such as ships and aircraft in view of cargo transportation or other reasons. These openings have caused significant fatigue problems. Carefully designed reinforcements of the edges of an opening can alleviate the local stress level around the opening, but a stress analysis by FE calculations should then be made.

On a much smaller scale, a hole in a plate element of a structure can be necessary for various arguments, usually related to passing of something through the hole. However, the stress concentration factor can easily be in the order of three or even higher for shear loading. Designers can apply a collar to the edge of the hole to reduce the stress level around the hole. Values of K_t for integral collars are presented in [1] and [4]. However, the variety of reinforcements around a hole is large in view of the method of joining the reinforcing material to the plate. Ring elements can be attached around the hole by fasteners (bolts, rivets) or adhesive bonding (in aircraft). It should be realized that the advantage of such reinforcements is not always obvious because fatigue critical locations can now occur at the edge of the reinforcement or fastener holes. Moreover, a high-stiffness reinforcement attracts load to the hole area and can also introduce bending due to the eccentricity of the reinforcement. Again, stress analysis as well as engineering judgement is required to deal with such problems.

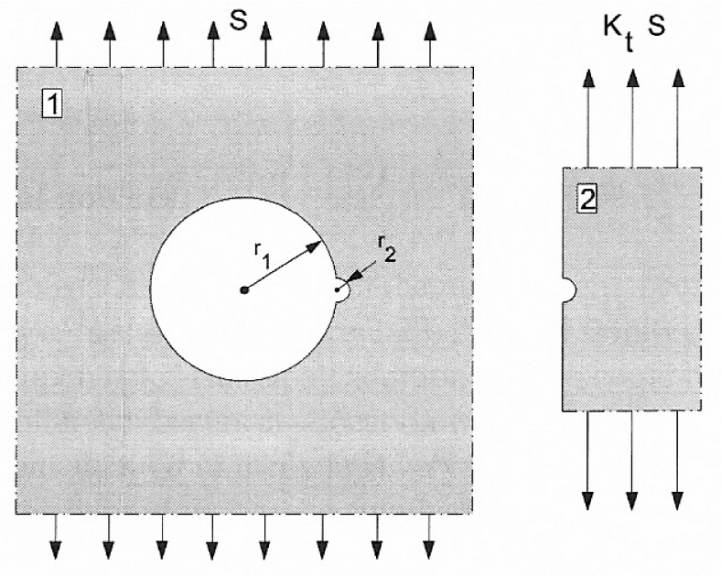

Fig. 3.23 Superposition of a very small notch on the root of a larger notch.

3.6 Superposition of notches

If a relatively small notch is added to the root of the main notch, there is a superposition of notches. A simple example is shown in Figure 3.23. A small semi-circular notch with $r_2/r_1 \ll 1$ occurs at the critical section of an open hole. This small additional notch could be mechanical damage inside the hole. The small notch occurs at a location where the peak stress would have been $K_{t1} \cdot S$. If the stress reduction away from the hole is still moderate, it can be assumed that the stress condition for the small notch is comparable to the second case shown in Figure 3.23. The K_t-value for this case is $K_{t2} = 3.07 \approx 3$, and the peak stress at the small notch added to the edge of the hole can be approximated by

$$\sigma_{\text{peak}} = K_{t1} K_{t2} S \quad \text{or} \quad K_t = K_{t1} K_{t2} \tag{3.14}$$

This is a reasonable first estimate if r_2 is much smaller than r_1. The K_t-value thus could be in the order of 9, which is very high. In reality, it will be lower because the small notch does not occur in a homogeneous stress field. Equation (3.14) will overestimate the real K_t. However, an amplification effect of the superposition will apply. This means that mechanical damage at the root of a notch can have a rather detrimental effect on the fatigue resistance.

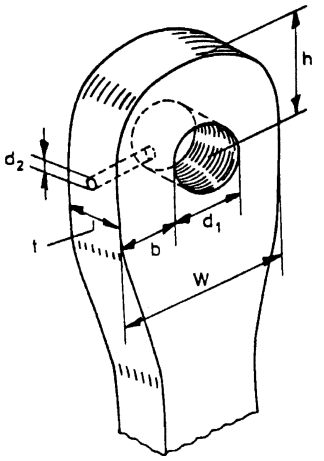

Fig. 3.24 Lug with a small lubrication hole to the lug hole. An example of superposition of two notches.

The above example refers to the superposition of an unintentional notch on another notch. This does not apply to the second example, shown in Figure 3.24. As discussed before, K_t for a lug is relatively high. In Figure 3.24, a superposition of notches occurs because of the small lubrication hole drilled to reach the main hole of the lug. Again Equation (3.14) will be a first approximation, and although it will be an overestimate, the total K_t-value will be very high. From a design point of view, the lubrication hole is entering the lug hole at the most unfavorable location. A much better solution would be to locate the lubrication hole at the top of the lug head. The two examples illustrate that a designer should try to avoid superposition of notches. If functional holes are necessary, this superposition effect can be limited by selecting appropriate positions in low-stress areas.

An other example of a superposition of notches is illustrated by Figure 3.25. It shows a fatigue crack in a bracket. A generous radius was applied between the vertical flange and the base plate. Unfortunately, the favorable radius was fully destroyed by machining a flat surface into the base plate to accommodate the positioning of an attachment bolt of the bracket. This caused a local superposition with a very sharp notch and fatigue cracking occurred in service. Such a mistake of detail design should be observed in the design office.

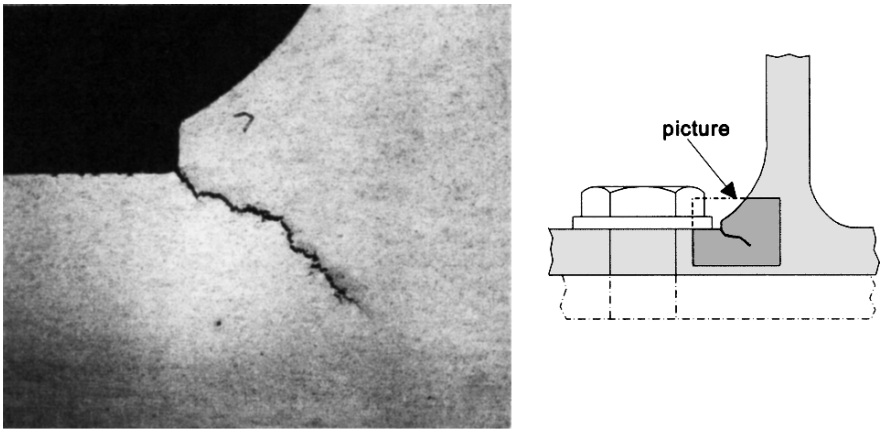

Fig. 3.25 Cross section of fatigue cracks at sharp corner.

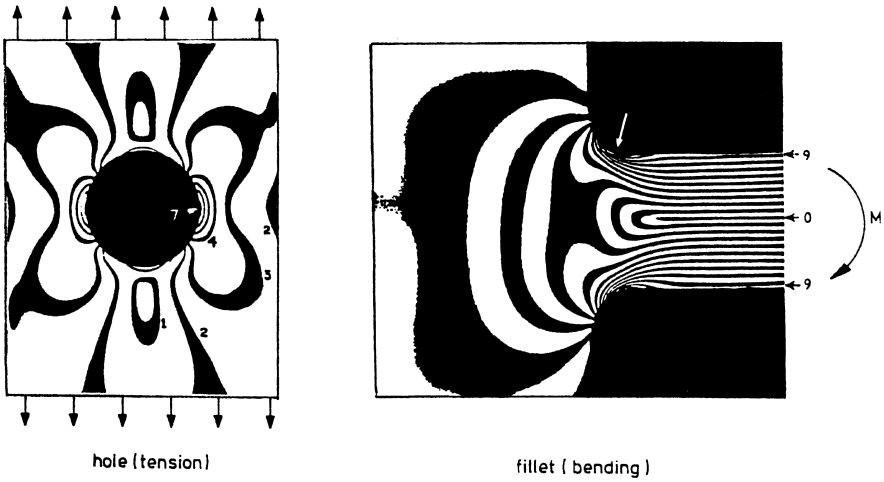

Fig. 3.26 Two examples of photo-elastic pictures [10].

3.7 Methods for the determination of stress concentrations

Before FE techniques were generally available, say before 1960, many K_t-values were obtained by measurements, e.g. by photo-elasticity [10, 11]. Various graphs in Peterson's book [1] are based on such measurements. Two pictures obtained by photo-elasticity are shown in Figure 3.26. The stress field can be derived from the black and white interference bands, called fringes. Local stresses can be obtained from the fringes as explained in [10, 11]. The parallel and equally spaced fringes in the thin section of

the fillet bending case illustrate the linear bending stress distribution across the thickness of the horizontal beam. Notice in this figure that the peak stress occurs at the transition of the beam to the very beginning of the fillet (see the arrow). In the past, the advantage of the photo-elastic method was that an impression of the entire stress field was obtained. Moreover, the photo-elastic model allows modifications of the shape to see how improved stress distributions can be obtained. However, the accuracy of the method is problematic.

An alternative measuring technique is to use strain gages. Strains can be measured fairly accurately. Strain gages with a small filament length should be used because of the large stress gradients at the notch. Such gages are available (gage length $\leq$ 1 mm). Unfortunately, the root of a notch is not always easily accessible for applying the strain gage. Accurate measurements of the peak stress are difficult. The strain gage technique is still used to measure nominal stress levels in full-scale structures or components.

It was pointed out before that similarity of notches (especially similar root radii) and superposition may be helpful to estimate K_t-values. Furthermore, interpolation between data for existing geometries is possible. Available data (e.g. [1]) should always be consulted to see whether information for similar geometries is available. However, the accuracy of several K_t graphs in the book by Peterson may be limited. More reliable K_t-values require a thorough elasto-mechanic analysis which in most cases will be FE calculations. An illustration of a simple FE model is given in Figure 3.27. The geometry of the component has to be modeled by a large number of small interconnected elements. Many more elements are required at places where stress gradients are high which generally applies to the area around a notch.

Nisitani and Noda [12] carried out calculations with the boundaryelement technique to obtain K_t-values for cylindrical bars with circumferential notches under tension, bending and torsion. They found K_t-values which were about 10% higher than data reported in the book by Peterson [1] which were based on a Neuber analysis. The authors found similar trends for strips with double and single edge notches [13]. Gooyer and Overbeeke [14] carried out FE calculations for a shaft with a shoulder fillet loaded under tension and torsion. They found K_t-values even more than 10% higher than reported in the book by Peterson. Similar discrepancies for shoulder fillets were obtained by Noda et al. [15].

An example of photo-elastic results compared to FE results is given in Figure 3.28 for four specimens with an increasing notch severity. Such specimens are used in laboratory experiments to study the fatigue notch

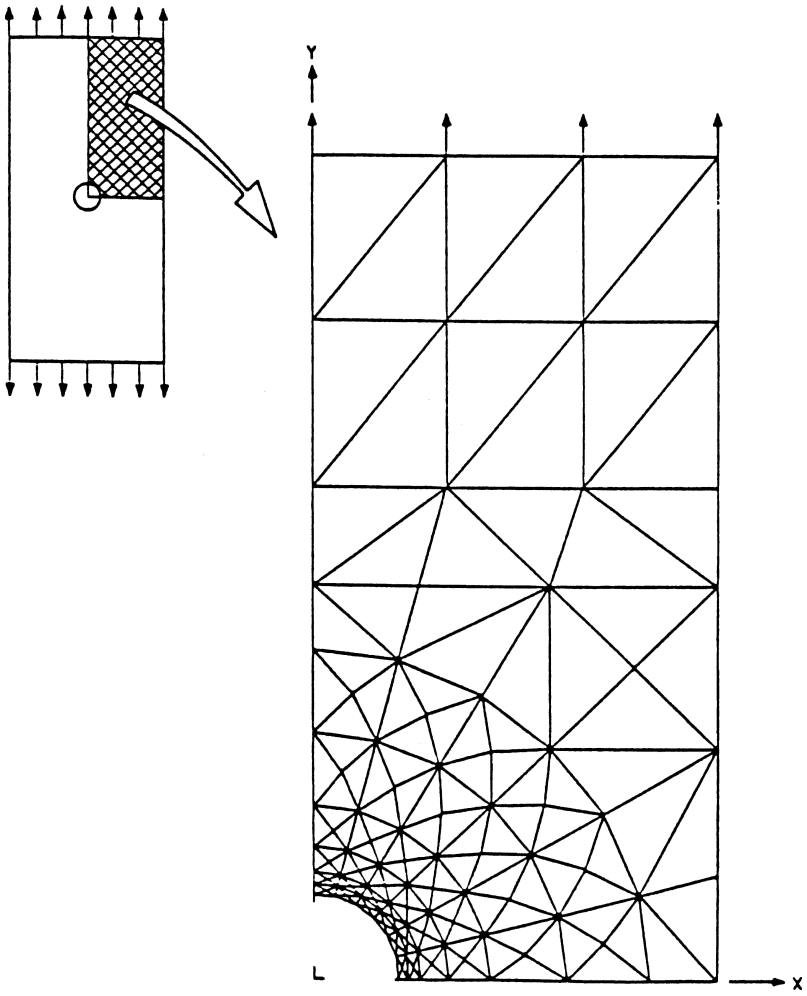

Fig. 3.27 Example of a FE model. In view of the symmetry of the load and the specimen, only one quarter needs to be modeled.

sensitivity of a material. The notch of specimen 3 consists of a circular hole with two semi-circular edge notches with a smaller radius (hole with ears). The notch of specimen 4 is obtained by drilling two small holes connected by a saw cut. This notch is the most severe one simulating a slit with rounded ends. The photo-elastic results confirm the increasing notch severity for specimens 1 to 4 in agreement with the trend of the FE results. Differences between the measured and calculated K_t-values are 10 to 16%. The calculated values should be expected to be more accurate.

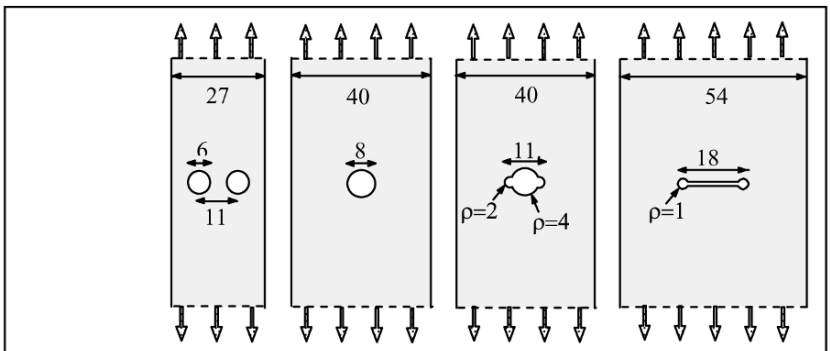

Case	1	2	3	4
K_t obtained by:				
Photo–elasticity	1.8	2.5	3.1	4.5
FE calculation	2.0	2.5	3.6	5.2
Estimation	2.17	2.51	3.47	5.36

Fig. 3.28 Comparison of K_t-values of notched specimens as obtained by photo-elastic measurements and FE calculations [16]. Estimated values are included. Dimensions in mm.

The bottom line of Figure 3.28 also gives estimated K_t-values obtained with simple approximations. Specimen 1 with two holes is replaced by a strip with a single hole and half the width of specimen 1. It leads to $D/W = 6/13.5$, and with the Heywood equation (Equation 3.12) the result is $K_t = 2.17$. The approximation for specimens 3 and 4 is obtained with the K_t equation for an elliptical hole (Equation 3.6b) with the semi-axis "a" equal to half the total width of the notch, and the same root radius at the end of the notch. This leads to K_t-values of 4.41 and 7.0 respectively for such holes in an infinite sheet. The width correction is assumed to be the same as for a circular hole according to the Heywood equation, implying a correction factor $\{2 + (1 - D/W)^3\}/3$. The K_t-values then become 3.47 and 5.36 respectively. A comparison with the FE results in Figure 3.28 shows that the estimates are reasonably accurate. The predominant significance of the notch root radius is thus emphasized again. It may also be pointed out that such K_t estimates are useful as a preliminary validation of FE calculations. It is desirable to have some idea about the magnitude of the value to be calculated.

For complex shapes, analytical calculation and estimates become impracticable. This certainly applies to components with a significant three-dimensional (3D) character, but also for 2D components with a

complex geometry, a limited symmetry and no comparable simple shapes. If stress concentration factors or stress distributions are needed, calculations should be made with finite element techniques for which several computer codes have been developed. Very satisfactory results can be achieved. FE calculations require experience and a critical view on the FE model adopted to simulate a component. Application of loads to the model, boundary conditions and mesh distributions should be given careful attention. It is useful to check computer programs by calculations on simple models for which solutions are already available.

The obvious criteria for a comparison between FE calculations and experimental techniques are: accuracy, cost-effectivity and time efficiency. If sufficient experience on FE calculations is available, the criteria are all in favor of the FE calculations. The computer also can provide colorful pictures of the stress distribution. Each color then corresponds to a certain interval of the stress level. Locations of peak stresses are easily recognized in such pictures. Complex shapes can be handled. Of course, it requires a computer program and a computer suitable for complex 3D problems. It is desirable to have experience with such calculations in order to understand what the computer program is doing.[7] Some strain gage measurements for the validation of the calculation may be useful if the full-scale structure is available for that purpose.

In practical problems, it should be questioned whether it is justified to spend substantial efforts on obtaining accurate K_t-values. Graphs in the book by Peterson with a limited accuracy can still give good indications of the reduction of K_t by increasing root radii. Moreover, it should be recognized that other input data required for fatigue life predictions may also be afflicted by uncertainties, e.g. the load spectrum. An other variable is scatter of root radii in production which can have a significant effect on K_t if small radii were specified on the production drawings.

3.8 Main topics of the present chapter

This section is not a summary of the present chapter, but the major results of the present chapter are recollected.

[7] It may be noted that the von Mises stress distribution is often calculated in FE programs. However, this is incorrect for a fatigue analysis for which the largest principal tensile stress is the most indicative stress component.

1. The most important variable for the stress concentration factor K_t is the root radius ρ. Sharp notches can give unnecessarily high K_t-values.
2. Loads applied close to the notch root usually give higher K_t-values than remotely applied loads.
3. Pin-loaded holes are a more severe stress raiser than open holes.
4. The gradient of the peak stress at the notch root to lower values away from the root surface ($\mathrm{d}\sigma_y/\mathrm{d}y$) is inversely proportional to the root radius ρ, and linearly proportional to the peak stress at the root of the notch, σ_{peak}. This gradient is relatively high and σ_y drops off rapidly away from the material surface. Contrary to this large gradient , the tangential stress along the material surface at the notch root decreases relatively slowly. This observation is significant for considering notch size effects on fatigue and notch surface qualities.
5. Superposition of notches can lead to a multiplication effect on K_t ($= K_{t1} \times K_{t2}$).
6. Accurate K_t-values can be calculated with FE techniques. With the current computers, these calculations are more accurate and cost-effective in comparison to measurements of stress distributions around notches.

References

1. Peterson, R.E., *Stress Concentration Factors.* John Wiley & Sons, New York (1974). New edition by Pilkey, W.D. and Pilkey, D.F., *Peterson's Stress Concentration Factors*, 3rd rev. edn., John Wiley & Sons (2008).
2. Timoshenko, S. and Goodier, J.N., *Theory of Elasticity*, 3rd edn.). McGraw Hill (1987).
3. Muskhelisvili, N.I., *Some Basic Problems of the Mathematical Theory of Elasticity*. Noordhoff (1963).
4. *Stress Concentration Factors.* ESDU Engineering Data, Structures, Vol. 7, Issued 1964 to 1995. Engineering Sciences Data Unit, London.
5. Schijve, J., *Stress gradients around notches*. Fatigue Engrg. Mater. Struct., Vol. 3 (1981), pp. 325–338.
6. Howland, R.C.J., *On the stress in the neighbourhood of a circular hole in a strip under tension*. Phil. Trans. Roy. Soc., Vol. 229 (1930), pp. 49–86.
7. Heywood, R.B., *Designing against Fatigue.* Chapman and Hall, London (1962).
8. Frocht, M.M. and Hill, H.N., *Stress concentration factors around a central circular hole in a plate loaded through pin in the hole*. J. Appl. Mech., Vol. 7 (1940), pp. A5–A9.
9. Frost, N.E., Marsh, K.J. and Pook, L.P., *Metal Fatigue.* Clarendon, Oxford (1974).
10. Heywood, R.B., *Designing by Photo-Elasticity.* Chapman and Hall, London (1952), and *Photo-Elasticity for Designers*. Pergamon Press (1969).
11. Durelli, A.J., Phillips, E.A. and Tsao, C.H., *Theoretical and Experimental Analysis of Stress and Strain.* McGraw-Hill (1958).

12. Nisitani, H. and Noda, N.-A., *Stress concentration of a cylindrical bar with a V-shaped circumferential groove under torsion tension or bending*. Engrg. Fracture Mech., Vol. 20 (1984), pp. 743–766.
13. Nisitani, H. and Noda, N.-A., *Stress concentration of a strip with double edge notches under tension or in-plane bending*. Engrg. Fracture Mech., Vol. 23 (1986), pp. 1051–1065. See also: *Engrg. Fracture Mech., Vol. 28* (1987), pp. 223–238 for a single edge notch.
14. Gooyer, L.E. and Overbeeke, J.L., *The stress distributions in shouldered shafts under axisymmetric loading*. J. Strain Anal., Vol. 26 (1991), pp. 181–184.
15. Noda, N.-A., Takase, Y. and Monda, K., *Stress concentration factors for shoulder fillets in round and flat bars under various loads*. Int. J. Fatigue, Vol. 19 (1997), pp. 75–84.
16. Ostermann, H., *Stress concentration factors of plate specimens for fatigue tests*. Laboratorium für Betriebsfestigkeit, LBF, Darmstadt, Report TM Nr. 61/71 (1971) [in German].

Some general references

17. Sih, G.C., *Stress Analysis of Notch Problems. Mechanics of Fracture, Vol. 5*. Noordhoff (1978).
18. Nisitani, H. (Ed.), *Computational and Experimental Fracture Mechanics.* Computational Mechanics Publications, Southampton (1994).
19. Leven, M.M., *Stress gradients in grooved bars and shafts.* Proc. SESA, Vol. 13 (1955), pp. 207–213.
20. Savin, G.N., *Stress distribution around holes.* NASA TT F-607 (1970) [translated from Russian].
21. Neuber, H., *Kerbspannungslehre.* Springer, Berlin (1937). Translation: *Theory of Notch Stresses.* J.W. Edwards, Ann Arbor, Michigan (1946).